phys. stat. sol. (b) **94**, 505 (1979)

Subject classification: 13.4; 22.1.2

Physikalisches Institut der Universität Würzburg (a)
and Natuurkundig Laboratorium der Universiteit van Amsterdam (b)

Iterative EHT Calculations for the Positive Divacancy in Silicon[1])

By

C. WEIGEL (a) and C. A. J. AMMERLAAN (b)

Iterative EHT calculations are carried out for the positive divacancy in silicon with an improved set of EHT parameters for silicon. The nearest neighbours of the divacancy are systematically displaced in the symmetry-allowed distortion modes until an acceptable agreement between calculated and experimentally derived wave function coefficients is reached for the nearest neighbours. At this particular distortion, the agreement for several shells of next-nearest neighbours also appears reasonable.

Iterative EHT-Rechnungen werden für die positive Doppelleerstelle in Silizium mit einem verbesserten Satz von EHT-Parametern ausgeführt. Die nächsten Nachbarn der Doppelleerstelle werden systematisch in Verzerrungsmoden, die von der Symmetrie erlaubt sind, versetzt, bis eine akzeptable Übereinstimmung zwischen berechneten und experimentell ermittelten Wellenfunktionskoeffizienten für die nächsten Nachbarn erreicht ist. Bei dieser bestimmten Verzerrung scheint die Übereinstimmung auch für mehrere Schalen von übernächsten Nachbarn vernünftig zu sein.

1. Introduction

Silicon is perhaps the most important of the elemental semiconductors, and many lattice defects in it have been studied both experimentally and theoretically. The defects can be classified according to their defect states as shallow or deep. For the shallow centres (most of the substitutional impurities), a general theory exists in the form of the effective mass theory [1] and its refinements [2].

Most of the lattice defects such as the divacancy are, however, deep. Contrary to the monovacancy, the divacancy is stable at room temperature and thus allows for extensive experimental studies. The divacancy can be observed in various charge states; among them, the positive one has, may be, the largest amount of detailed experimental evidence available. Infrared absorption measurements [3] show that the singly occupied energy level of the positive divacancy lies 0.25 eV, at most, above the valence band edge. Hyperfine interactions giving information about the defect electron wave function have first been observed in EPR [4] and then, with greater resolution, in ENDOR [5]. These experiments reveal that the point symmetry of the defect is C_{2h}, which is the result of a Jahn-Teller distortion of the environment of two adjacent lattice sites having D_{3d} symmetry in the perfect lattice.

A theoretical treatment must therefore take into account the proper charge state and symmetry of the divacancy. This defect thus constitutes an excellent testing ground for any theoretical approach that tries to overcome the absence of a general theory for deep defects.

[1]) Work supported in part by the Deutsche Forschungsgemeinschaft and the Office of Naval Research (USA) under Contract No. 00014-75-C-0919.

The calculations of Callaway and Hughes in the Green's functions formalism [6] are for the neutral charge state and do not incorporate any lattice distortions. Lee and McGill [7] do incorporate lattice distortions in their calculations employing the extended Hückel theory (EHT) [8], which is a semi-empirical, non-self-consistent LCAO approach. They do not, however, consider distortion modes of E_g symmetry as required by group-theoretical arguments. Rather, they displace the six nearest neighbours (nn's) according to the ad hoc imposition that one of the three unbroken bonds of each nn is stretched and the other two are bent. They place the divacancy in the centre of a 64 atom unit cell and then repeat this cell periodically. The advantage of this molecular unit cell approach (MUCA) consists in the absence of perturbing surface effects.

Our previous divacancy calculations [9] use the same approach (MUCA), but we investigated systematically the E_g-type distortions of the six nn's to achieve a best possible agreement of the calculated hyperfine tensors with experimental ones. Good agreement was obtained for the first nn's, while only some tentative assignment of calculated to measured hyperfine tensors could be made for next nn atoms.

A possible way to improve the theoretical treatment of the divacancy is to incorporate charge dependence in the calculations, which would entail an iterative scheme. This is, however, difficult to do in the MUCA, which is essentially a band structure scheme with a very large unit cell. The results consequently depend on the k-vector. An additional problem of MUCA has to do with the relative closeness of the defects in the unit cells. Due to their periodical repetition, one does not really study an isolated defect, but rather, as it were, a defect superlattice (cf. [10]). We therefore carried out iterative EHT calculations for clusters of silicon atoms with two vacant lattice sites.

In Section 2 we will describe the clusters, and in Section 3 the iterative EHT scheme together with the parameters that enter into it. Section 4 contains the results, while possible improvements are discussed in Section 5.

2. Model Clusters

In smaller clusters (up to 20 atoms), most of the atoms are essentially surface atoms; one then really deals with a molecule which has little to do with an extended solid. Earlier EHT cluster calculations (see, e.g., [11]) have shown that model clusters containing 30 atoms, at least, are necessary such that the resulting energy levels group themselves into what can be considered as a valence and a conduction band of a solid.

One might then expect that the simulation of a solid improves systematically with the number of atoms in the cluster. But we did some test calculations showing that, as the number of atoms in the clusters increases (> 90 atoms), surface states due to the growing number of broken bonds are beginning to creep into the energy gap, which leads to spurious results.

Clusters with numbers of atoms ranging between 50 and 80 appear to strike a reasonable compromise in view of the above considerations. We did most of the calculations in a 68 atom cluster, which lies in this region of reasonable compromise and has D_{3d} symmetry like the undistorted divacancy.

In keeping with the geometric arrangement adopted in previous experimental and theoretical work, we place the divacancy and nn sites at the positions listed in Table 1. These coordinates are given in units of 0.6785 Å, which is one eighth of the non-primitive f.c.c. lattice constant of silicon. Table 2 shows the symmetry relations between the six nn atoms under the four operations of the C_{2h} group, namely E (identity), C_2 (twofold rotation), σ_h (reflection), and i (inversion). Atoms 1 and 2 form

Table 1

coordinates		x	y	z
divacancy sites		1	−1	−1
		−1	1	1
six	(1)	1	3	3
nearest-	(2)	−1	−3	−3
neighbour	(3)	−3	−1	3
sites	(4)	−3	3	−1
	(5)	3	1	−3
	(6)	3	−3	1

Table 2

Symmetry relations between the six nn's under C_{2h} operations

E	C_2	σ_h	i
1	2	1	2
2	1	2	1
3	6	4	5
4	5	3	6
5	4	6	3
6	3	5	4

a mirror-plane shell; they are transformed into themselves. Atoms 3, 4, 5, and 6 form a general-class shell. Table 3 lists representative atoms for the remaining mirror-plane and general-class shells of the model cluster.

We have to consider two distortions that transform according to the E_g irreducible representation of D_{3d}. This follows from two points:

One point is that the uppermost occupied state of the positive divacancy is an E_u state, and that according to the Hellmann-Feynman theorem [12] the symmetry is lowered by distortions belonging to irreducible representations contained in the symmetrized product $|E_u \times E_u|$ which is $A_{1g} + E_g$. Of these two representations, only E_g can lower the symmetry.

The other point concerns the number of linearly independent E_g distortions. The six nn's are capable of 18 normal-mode distortions including translations and rotations. Among them are three E_g modes. Since one of them represents a pure rotation, there are two E_g modes left to consider for a specified orientation of the mirror plane.

The distortions are shown in Fig. 1. We define a distortion mode to have a magnitude of 1 if the rms displacement of the six nn's is 1 Å. To be specific, we give the displacement vectors for atoms 1 and 3 in the same scale as in Table 1:

	atom	EG1 distortion	EG2 distortion
(1)	(1, 3, 3)	(1.203, 0.602, 0.602)	(0.188, −1.315, −1.315)
(3)	(−3, −1, 3)	(−0.602, 0.602, −1.203)	(−1.221, 0.094, 0.094)

Table 3

Representative atoms of the shells in the model cluster

mirror-plane shells			general-class shells		
1	3	3	−3	−1	3
7	1	1	3	5	1
−1	5	5	1	3	−5
9	−1	−1	5	3	−1
7	−3	−3	1	−1	7
9	3	3	−5	5	1
7	5	5	−1	1	9
			−3	3	7
			5	3	7
			−3	−5	7
			−3	−9	3
			−7	−5	3
			−5	−7	5

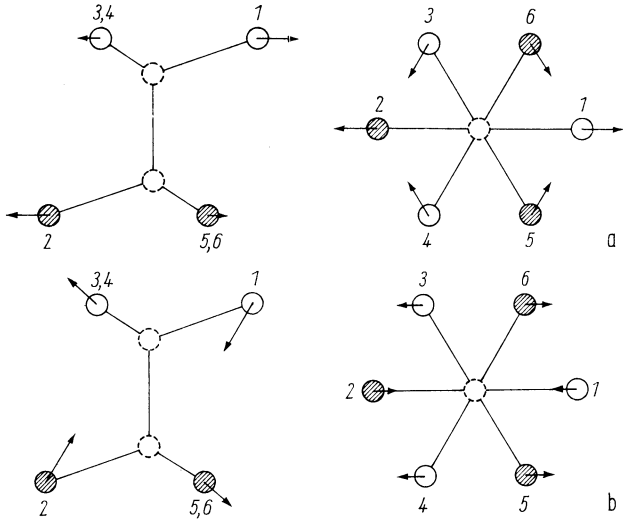

Fig. 1. Distortion modes a) EG1 and b) EG2. Broken circles indicate vacant sites; for the positions of the six nn's see Table 1. The arrows are for an rms displacement of 1 Å

3. Iterative EHT

EHT is an approximation to the rigorous Hartree-Fock-Roothaan (HFR) theory [13]. In EHT, one has to solve the secular equations which have the same form as in HFR, namely

$$\sum_{\nu} (H_{\mu\nu} - E_i S_{\mu\nu})\, c_{\nu i} = 0 \tag{1}$$

for the eigenvalues, E_i, and the coefficients, $c_{\mu i}$, for the expansion of the eigenfunctions φ_i in the atomic basis functions, χ_μ:

$$\varphi_i = \sum_{\mu} c_{\mu i} \chi_\mu \,. \tag{2}$$

The overlap integrals $S_{\mu\nu} = \langle \chi_\mu \mid \chi_\nu \rangle$ are the same as in the HFR theory, but the Hamiltonian matrix elements are greatly simplified:

$$\left.\begin{aligned} H_{\mu\nu} &= -I_\mu \,; \qquad \mu = \nu \,, \\ &= S_{\mu\nu} K_{\mu\nu} - (I_\mu - I_\nu)/2; \quad \mu \neq \nu \,. \end{aligned}\right\} \tag{3}$$

The I_μ's are ionization energies of the atomic states, χ_μ, of the free atoms and the constants $K_{\mu\nu}$ are purely empirical parameters. Since the basis functions χ_μ are centered on the atoms, the overlap integrals $S_{\mu\nu}$ incorporate the geometry of the system, in particular the nn distortions, into the calculations.

As atomic basis states, we take one 3s and three 3p orbitals and represent them as Slater-type orbitals (STO's), which are characterized by orbital exponents ζ. Table 4

Table 4
Orbital coefficients ζ and K values

reference	ζ(3s)	ζ(3p)	$K_{ss} = K_{pp}$	K_{sp}
Messmer and Watkins [16]	1.87	1.60	1.75	1.313
Clementi and Raimondi [17]	1.634	1.428	1.75	1.75
present work	1.90	1.428	1.75	1.46

contains the orbital exponents of the STO's used in our calculations together with the $K_{\mu\nu}$ values.

In the non-iterative scheme, the $H_{\mu\nu}$'s are obviously independent of the net charges sitting on the atoms. These charges are calculated only afterwards, which can be done by carrying out a Mulliken charge population analysis [14]. If an eigenstate φ_i carries n_i electrons ($n_i = 0$, 1, or 2), then this charge is distributed over the atomic basis states such that a state χ_μ holds a charge $q_{\mu i}$:

$$q_{\mu i} = -n_i c_{\mu i} \sum_\nu S_{\mu\nu} c_{\nu i} \,. \tag{4}$$

The total charge q_A (expressed in units of $|e|$) sitting on an atom is obtained by summing over all χ_μ's that are centered on that particular atom A, and over all i's:

$$q_A = \sum_{\mu \text{ on A}} \sum_i q_{\mu i} \,. \tag{5}$$

The next step in the procedure is to make the I_μ's dependent on q_A or rather on its deviation from the neutral value q_A^0, namely $\Delta q_A = q_A - q_A^0$. The neutral value q_A^0 is $-(4 + b)$, where b is the number of broken bonds for the particular atom. We have followed the work of Basch et al. [15], where the I_μ's are expanded in powers of Δq_A like

$$I_\mu(\Delta q_A) = A(\mu)\,(\Delta q_A)^2 + B(\mu)\,\Delta q_A + C(\mu) \,. \tag{6}$$

The coefficients are (in eV)

$$A(3s) = 1.62\,, \qquad B(3s) = 12.38\,, \qquad C(3s) = 14.95;$$

$$A(3p) = 1.61\,, \qquad B(3p) = 10.13\,, \qquad C(3p) = \;\; 7.77\,.$$

With these new values according to (6), one would set up new $H_{\mu\nu}$'s (equation (3)), solve (1) and (2), calculate new charges, compare with the old ones, and repeat everything until convergence in the charges is achieved.

Experience shows that it is almost impossible to achieve convergence if simply the newly calculated I_μ's are taken as starting points for the next step. The variations are too great and often lead to oscillatory behaviour of the charges as the iterations continue.

This difficulty can be overcome by introducing a damping parameter λ, reducing the magnitude of the correction due to the newly calculated charges:

$$I_\mu^{\text{new}} = I_\mu^{\text{old}}(1 - \lambda) + \lambda[A(\mu)\,(\Delta q_A)^2 + B(\mu)\,\Delta q_A + C(\mu)] \,. \tag{7}$$

We chose λ to be of the order of 0.1 and terminated the iterations when the difference between the q_A's from successive iterations was less than 0.005 for every atom. Convergence of that sort was generally reached after seven iterations.

We should remark at the end of this description that an EHT scheme with iterations on charges is still not self-consistent, as Harris has pointed out [18], although he cannot state, either, whether great practical differences between the results of a charge-iterative and a self-consistent scheme exist.

4. Results

4.1 Initial calculations

The interaction between the electron in the defect state φ with spin $\boldsymbol{S}$ and a nucleus with nuclear spin $\boldsymbol{I}$ is described by the spin Hamiltonian H_S:

$$\langle\varphi|\, H_S \,|\varphi\rangle = \boldsymbol{S} \cdot \mathbf{A} \cdot \boldsymbol{I} \,. \tag{8}$$

A is the hyperfine interaction tensor, which can be decomposed as

$$\mathbf{A} = a\mathbf{1} + \mathbf{B} . \tag{9}$$

The isotropic part is known as the Fermi contact term with

$$a = \tfrac{8}{3}\pi g\beta g_N\beta_N |\varphi(0)|^2 , \tag{10}$$

where 0 refers to the position of the nucleus.

The elements of the anisotropic tensor **B** are

$$B_{ij} = g\beta g_N\beta_N \langle\varphi| (3x_ix_j - r^2\delta_{ij})/r^5| \varphi\rangle . \tag{11}$$

They are known as dipole–dipole tensor elements due to the analogous formula for the interaction of two classical dipoles.

The components of the different hyperfine interaction tensors thus permit the calculation of wave function coefficients of the defect wave function φ:

$$\begin{aligned}\varphi &= \sum_\mu c_\mu\chi_\mu \\ &= \sum_r \sum_i [\alpha_{ri}\chi(3s)_{ri} + \beta^x_{ri}\chi(3p_x)_{ri} + \beta^y_{ri}\chi(3p_y)_{ri} + \beta^z_{ri}\chi(3p_z)_{ri}] .\end{aligned} \tag{12}$$

The index i runs over the atoms of a shell indicated by r.

If one comes from the experimental results, the index r just stands for a so far undefined shell of atoms. We now want to identify these shells.

An earlier work [19] reporting the results of [5] contains experimentally derived coefficients in the form α^2 and $\beta^2 = (\beta^x)^2 + (\beta^y)^2 + (\beta^z)^2$ These values are given in Table 5.

It is certainly reasonable to assume that the greatest contributions to the defect function come from the six nn's of the divacancy. Therefore, we tried to find such combinations of EG1 and EG2 distortions that the α^2 and β^2 values came as close as possible to the M1 and G1 values in Table 4. The shell consisting of atoms 3 through 6 was identified with G2 in [4]. Therefore, also G2 is a candidate for the match as we will see in Section 4.3. For these preliminary calculations we varied EG1 between 0.1 and 0.25 and EG2 between 0.05 and 0.15, since our MUCA calculations had yielded reasonable results in this range. We also used the same EHT parameters, viz. those proposed by Messmer and Watkins [16] (see Table 4).

Table 5

Experimentally derived wave function coefficients (in %) for the defect function of the positive divacancy [19]

mirror-plane class			general class		
	α^2	β^2		α^2	β^2
M1	3.6	27.7	G1	0.544	1.917
M2	0.359	2.738	G2	0.463	0.621
M3	0.131	0.883	G3	0.246	1.592
M4	0.076	0.389	G4	0.170	1.005
M5	0.061	0.508	G5	0.086	0.347
M6	0.032	0.228	G6	0.052	0.334
M7	0.024	0.048	G7	0.043	0.311
			G8	0.039	0.247
			G9	0.039	0.242
			G10	0.020	0.092
			G11	0.015	0.094
			G12	0.013	0.080

The results of these preliminary calculations were not very satisfactory. To be true, the α^2 and β^2 values for the six nn's turned out to be in the correct order of magnitude of the M1 and G1 values (Table 5). But the α^2's and β^2's were, in general, too small.

This raised the possibility that the set of EHT parameters used is not the optimal one. To see what changes would result from using other sets of available EHT parameters for silicon, the set due to Clementi and Raimondi [17] (see Table 3) was used in the calculations with the following general results: The α^2's were even smaller, i.e. worse as compared with the experimentally derived values, whereas the agreement for the β^2's became much better.

These findings are reasonable considering that a larger orbital exponent renders a wave function more concentrated around its centre and vice versa. Thus a change for the ζ(3s) exponent from 1.87 to 1.634 makes the function more diffuse and reduces the Fermi contact term which determines α^2. Likewise a smaller ζ(3p) exponent makes the wave function more extended in space such that the dipole–dipole term increases and consequently β^2, too.

The preliminary results gave therefore the motivation for an attempt to obtain an improved set of EHT parameters for silicon. The following part describes this new set, in which ζ(3s) is larger than the value used by Messmer and Watkins and ζ(3p) is lower than theirs.

4.2 Improved EHT parameter set for silicon

If a set of EHT parameters is supposed to yield reasonable results for defect states in a certain substance, then it must also be able to describe the electronic structure of the defect-free substance in an adequate manner. Therefore, the energy band structure for the infinite perfect solid should have as many properties as possible in agreement with experiment and/or other, more exact theoretical results.

The EHT parameters were then changed according to the ideas outlined in Section 4.1. They were also adjusted so as to yield an indirect band gap in close agreement with the exeprimental value of 1.13 eV [20]. The set of EHT parameters that emerged from these adjustments is listed in Table 4, and the band structure that was calculated with the parameters is shown in Fig. 2.

This band structure has an indirect gap of 1.1 eV; the minimum of the conduction band at the k-vector (0.6, 0, 0) lies, however, somewhat off the experimentally determined minimum position of (0.85, 0, 0) [21]. The valence band width is 12.8 eV as compared to the experimental value of about 12.5 eV [22]. Other energy differences have reasonable values, too. The difference between $\Gamma_{25'}$ and L_1 in the conduction band is 1.4 eV (cf. 1.57 eV [23]) and the direct gap at L between $L_{3'}$ and L_1 is 3.1 eV (cf. 3.4 eV [24]).

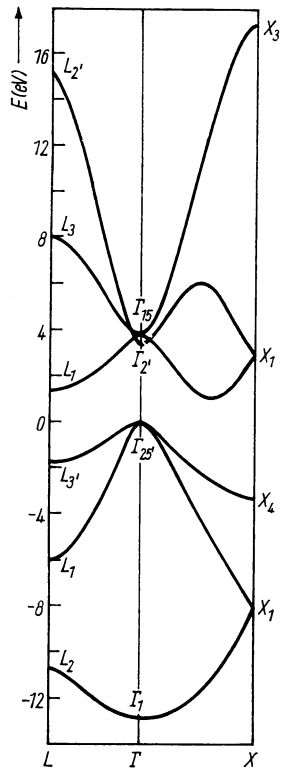

Fig. 2. Electronic energy band structure for silicon calculated by EHT with the parameters listed in Table 4. The energy of the top of the valence band has been set to zero

As for the direct gap at Γ, it was uncertain for a long time as to whether the lowest conduction band is $\Gamma_{2'}$ or Γ_{15}, although there was agreement that the bands are quite close (see, e.g., the various band structure results listed in [25]). Newer experiments have shown that Γ_{15} is lower than $\Gamma_{2'}$ [26].

Recent theoretical calculations determine the energy differences as $\Gamma_{2'} - \Gamma_{25'} = = 3.7$ eV and $\Gamma_{15} - \Gamma_{25'} = 3.1$ eV [27]. Our results are in the reverse order, but are generally in the correct order of magnitude: $\Gamma_{2'} - \Gamma_{25'} = 3.2$ eV, $\Gamma_{15} - \Gamma_{25'} = = 3.8$ eV. Considering that, after all, EHT is a relatively simple method, these results are not bad, which can also be said for the elastic constants. We calculated them following the method described by Watkins and Messmer [28]. The results are listed in Table 6, together with the constants calculated with the parameters due to Messmer and Watkins [16]. Since the value of c_{12} is derived from the bulk modulus $B = = \frac{1}{3}(c_{11} + 2c_{12})$, we rather list the results for B.

Apart from our c_{11} value, which is slightly worse than the value due to the parameters of Messmer and Watkins, our B and c_{44} values are definitely better.

In summary, the new set of EHT parameters yields a band structure which still leaves room for improvement, but which, nevertheless, has better properties than previously obtained band structures calculated by the same (simple) EHT approach.

Table 6
Elastic constants of silicon (in 10^{11} Pa)

	c_{11}	B	c_{44}
experimental [29]	1.66	0.979	0.796
calculated with parameters of Messmer and Watkins [16]	0.85	−0.085	0.235
calculated with present parameters	0.79	1.16	0.65

4.3 Divacancy calculations with the improved EHT parameters

As described in Section 4.1, we first tried to obtain an acceptable agreement between experimentally derived and calculated α^2 and β^2 values for the six nn's; in Fig. 3a and 3b we show how these values change for some variations in the distortion modes EG1 and EG2.

Ideally, for a certain combination of EG1 and EG2 distortions, all the calculated values would coincide with some experimentally derived values represented by horizontal lines in the figures such that an unambiguous assignment could be made.

This is clearly not the case. Inspection of these figures shows that an improvement in one value would be accompanied by a deterioration for another value. Also, it does not appear reasonable to extend the investigations to more EG1 values than the ones used between 0 and 0.2, and other EG2 values than those between 0.05 and 0.1. It may appear that smaller EG2 values would improve the β^2 values for the atoms (1, 3, 3) and (−3, −1, 3), but there the ordering of the defect levels in the gap is such that an A_u state rather than a B_u level would be filled with one electron. This A_u level would have no s-character in the mirror plane, and hence α^2 would vanish for the first nn in the mirror plane, in particular, which contradicts the experimental results.

A combination of EG1 ≈ 0.15 and EG2 ≈ 0.075 appears as an acceptable compromise, which yields reasonable values for all nearest-neighbour atoms; this is, by the way, also in agreement with our findings based on the MUCA calculations. The values corresponding to this particular distortion are indicated by crosses in the plots.

As was indicated in Section 4.1, a clear assignment of the (−3, −1, 3) shell to either G1 or G2 cannot be made, although G1 appears as the better candidate. It is then not

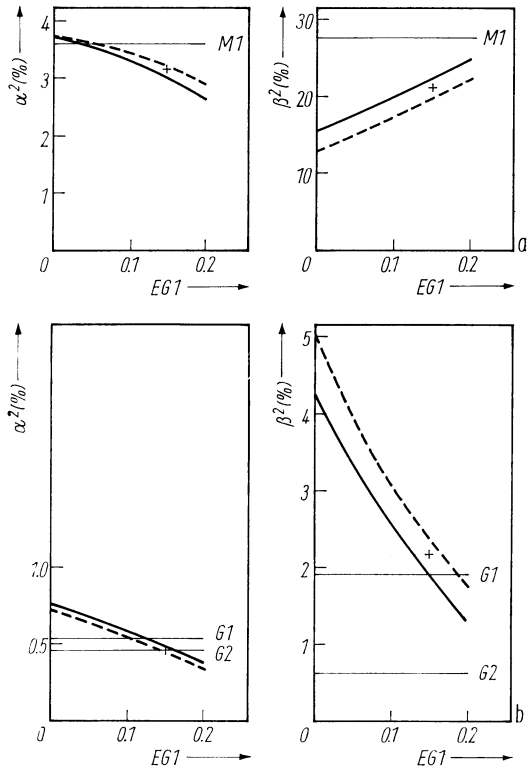

Fig. 3. a) Defect wave function coefficients for the mirror-plane atom (1, 3, 3). Here, as in all subsequent figures, the solid line refers to EG2 = 0.05 and the dashed line to EG2 = 0.1, while the crosses refer to (EG1, EG2) = (0.15, 0.075). b) Defect wave function coefficients for the general-class atom (−3, −1, 3)

possible to find another shell for G2 since for no next nn shell the α^2 and β^2 values are close to the G2 values at the same time (see below).

For the next nn's, we have plotted only those α^2 and β^2 curves which lie in the order of magnitude of the experimentally derived values of M2, M3, G2, G3, G4, G5, and G6 (Fig. 4a and 4b). Since, as we will see, the assignment of shells of atoms to experimentally derived shells is already getting more and more difficult, the problem is practically impossible to solve for the remaining shells of atoms.

The α^2 value for the (−1, 5, 5) mirror-plane atoms lies near the experimental M2 value, while there is a big discrepancy between the calculated and the experimental β^2 values. A closer inspection of the model reveals that the (−1, 5, 5) atoms are not completely surrounded by other atoms, but rather have one dangling bond, a situation which always makes the results for such atoms less reliable.

A calculation for the particular distortion described above was carried out in a 98 atom cluster, where the (−1, 5, 5) atoms are not located at the cluster surface. The results for this calculation are indicated by circles in Fig. 4a. On the basis of these results, an assignment of the (−1, 5, 5) atoms to shell M2 or M3 appears plausible, which is in agreement with the results of our MUCA calculations. The situation for the atoms of this particular mirror plane could probably be further clarified if more than just first nn atoms are distorted (see also Section 5).

As for the general-class atoms, the (5, 3, −1) atom shell is a very good candidate for the G4 shell (see Fig. 4b). The assignment of the (3, 5, 1) atoms to the G3 shell appears only slightly less certain. Only the values for the (−5, 5, 1) atoms do not lie near the experimental values for one and the same shell. For these atoms, however, the same surface problem exists as for the (−1, 5, 5) atoms. The already mentioned calculation for EG1 = 0.15 and EG2 = 0.075 in the 98 atom cluster then yielded the values indicated by circles in Fig. 4b, which suggests an assignment of the (−5, 5, 1) atoms to the G5 or G6 shell. The assignment with G5 was also suggested on the basis of our MUCA calculations.

As far as the energy levels in the gap are concerned, we must remark that the gap for the 68 atom cluster is larger than the experimental gap. This type of discrepancy occurs in every calculation with finite clusters (cf., e.g., [11]). This has to do

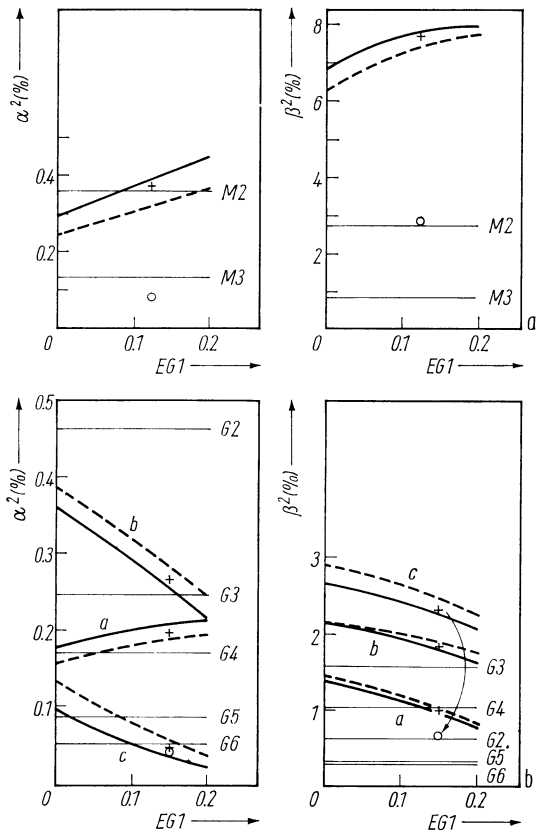

Fig. 4. a) Defect wave function coefficients for the mirror-plane atom (−1, 5, 5) (for the circles, see text). b) Defect wave function coefficients for the general-class atoms: (a) (5, 3, −1), (b) (3, 5, 1), and (c) (−5, 1)

with the general observation that the conduction band states are reproduced worse than the valence band states. The divacancy states lie, however, close to the valence band (for the positive charge state) such that this cautioning remark should apply to a lesser degree. We then note that in the 68 atom cluster the singly occupied B_u state lies 0.35 eV above a doubly occupied A_g state, which is the uppermost of all valence band states. We remember that the defect level of the positive divacancy lies 0.25 eV above the valence band edge, such that we can speak of a qualitative agreement, considering the accuracy of our calculations. This, again, applies for the particular distortion of EG1 = 0.15 and EG2 = 0.075, where the unoccupied remaining levels in the gap lie at 0.42 eV (A_u), 0.55 eV (B_g), and 0.56 eV (A_g) above the doubly occupied A_g state. All these gap levels display relatively little dispersion over the range of the distortions considered (see Fig. 5).

Fig. 6 shows size and direction of the p-orbitals on the nn's contributing to the defect state. These p-orbitals are responsible for the directions of the broken bonds on the respective atoms.

The position of the nn's are those for the particular distortion, where EG1 = 0.15 and EG2 = 0.075. The actual displacements are quite small and about the length of the radius of the circles symbolizing the nn's.

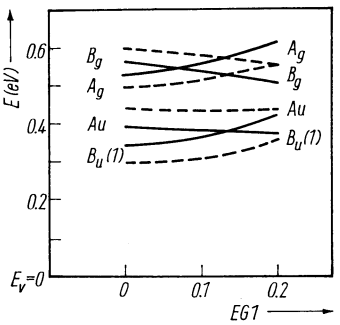

Fig. 5. The energy gap levels of the positive divacancy (one electron in the B_u state) calculated for various distortions. Solid curves: EG2 = 0.05; dashed curves: EG2 = 0.1. E_V = = 0 refers to the energy of the uppermost of the valence band states, which is practically constant for the distortions considered

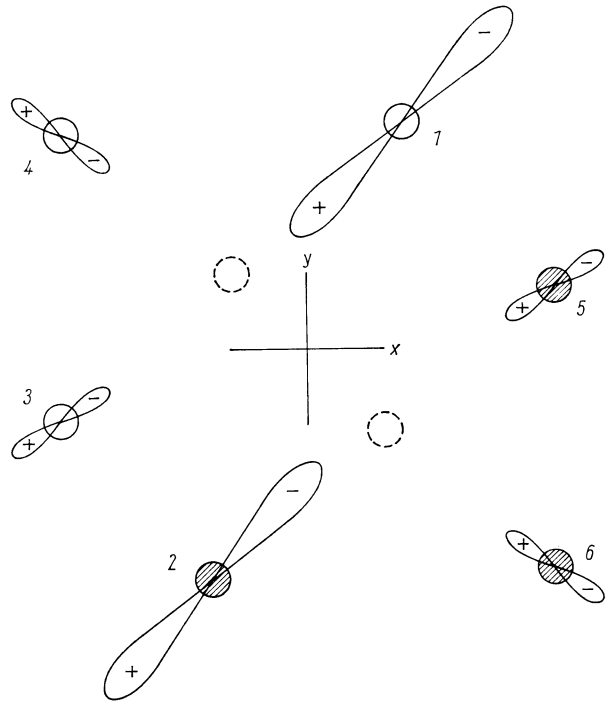

Fig. 6. Contribution of the p-orbitals on the six nn's of the divacancy to the defect state. The size of the lobes is meant to indicate the strength of the contribution. The positions of the six nn's correspond to the distortion (EG1, EG2) = (0.15, 0.075)

The general-class atoms 3 and 4 (likewise 5 and 6) have moved closer to each other; phase and direction of the orbtials on them indicate bonding combinations. The mirror-plane atoms 1 and 2 have moved away from each other. Their orbitals do not point directly to the nearest vacant site, but into a direction shifted towards the other mirror-plane atom.

These features of the nn's and the defect function derived from our calculation are in agreement with the microscopic picture for the divacancy developed in [4] on the basis of EPR measurements. Our calculations thus confirm the model of [4].

5. Possible Improvements within This Framework

As we assess the merits of these calculations, we can state with a certain degree of confidence that the assignment of several shells of divacancy neighbour atoms to experimental hyperfine tensors has become possible for the first time, or has received added credibility if such an assignment was already done based on our earlier MUCA calculations.

The added credibility stems, for one, from the fact that the EHT parameters employed yield an electronic band structure for silicon, which is better in several aspects than any other band structure calculated so far by EHT, although this band structure certainly leaves still room for improvement.

Another point is that for the first time we could carry out a calculation explicitly for the *positive* divacancy. This is due to our method which iterates on charges. This makes it worthwhile to consider an analogous treatment of the negative divacancy, for which information about the defect electron wave function due to ENDOR experiments is available, too [30].

But for now, we could also try to improve on the present calculations by taking further allowed types of distortions of divacancy neighborus. We remember that, so

far, only E_g-type distortions of the first six nn's were considered. We can still apply A_{1g}-type distortions, which would not alter the symmetry of the six nn's, but rather uniformly enlarge or decrease the geometry of these six atoms. There are two possible types of A_{1g} distortions, which would entail a considerable amount of calculations if the two E_g's were combined with them. We did therefore not consider them here; in addition, our MUCA calculations showed that the A_{1g} distortions caused relatively minor modifications of the results based on the E_g distortions alone.

Finally, second and further nearest neighbours should be displaced in both E_g- and A_{1g}-type distortions, because there is no plausible reason why only first nn's should be distorted. It is, however, easy to see that there is a large number of possible distortion types to consider, and that there is no simple way how to start a systematic study of them.

References

[1] J. M. LUTTINGER and W. KOHN, Phys. Rev. 97, 869 (1955).
W. KOHN, Solid State Phys. 5, 257 (1957).
[2] S. T. PANTELIDES and C. T. SAH, Phys. Rev. B 10, 621, 638 (1974).
[3] H. Y. FAN and A. K. RAMDAS, J. appl. Phys. 30, 1127 (1959).
[4] G. D. WATKINS and J. W. CORBETT, Phys. Rev. 138, A543 (1965).
[5] J. G. DEWIT, E. G. SIEVERTS, and C. A. J. AMMERLAAN, Phys. Rev. B 14, 3494 (1976).
[6] J. CALLAWAY and A. J. HUGHES, Phys. Rev. 164, 1043 (1967).
[7] T. F. LEE and T. C. MCGILL, J. Phys. C 6, 3438 (1973).
[8] R. HOFFMANN, J. chem. Phys. 39, 1397 (1963).
[9] C. A. J. AMMERLAAN and C. WEIGEL, Conf. Radiation Effects in Semiconductors, Dubrovnik 1976, Inst. Phys., London 1977 (p. 448).
[10] R. P. MESSMER and G. D. WATKINS, Conf. Radiation Damage and Defects in Semiconductors, Reading 1972, Inst. Phys., London 1973 (p. 255).
[11] R. P. MESSMER and G. D. WATKINS, Phys. Rev. B 7, 2568 (1973).
[12] H. HELLMANN, Quantenchemie, Deuticke, Leipzig 1937 (p. 285).
R. P. FEYNMAN, Phys. Rev. 56, 340 (1939).
M. D. STURGE, Solid State Phys. 20, 91 (1967).
[13] C. C. J. ROOTHAAN, Rev. mod. Phys. 23, 69 (1951).
[14] R. S. MULLIKEN, J. chem. Phys. 23, 1833 (1955).
[15] H. BASCH, A. VISTE, and H. B. GRAY, Theor. Chim. Acta (Berlin) 3, 458 (1965).
[16] R. P. MESSMER and G. D. WATKINS, unpublished results (1972).
[17] E. CLEMENTI and D. L. RAIMONDI, J. chem. Phys. 38, 2686 (1963).
[18] F. E. HARRIS, J. chem. Phys. 48, 4027 (1968).
[19] J. G. DE WIT, Thesis, Univ. Amsterdam, 1975 (unpublished).
[20] A. FROVA and P. HANDLER, Phys. Rev. Letters 14, 178 (1965).
[21] G. FEHER, Phys. Rev. 114, 1219 (1959).
[22] L. LEY, S. KOWALCZYK, R. POLLAK, and D. A. SHIRLEY, Phys. Rev. Letters 29, 1088 (1972).
W. D. GROBMAN and D. E. EASTMAN, Phys. Rev. Letters 29, 1508 (1972).
V. G. ALESHIN and YU. N. KUCHERENKO, Izv. Akad. Nauk SSSR, Ser. fiz. 40, 311 (1976).
[23] J. METZDORF and F. R. KESSLER, Verh. DPG (VI) 12, 95 (1977).
[24] R. R. L. ZUCCA, J. P. WALTER, Y. R. SHEN, and M. L. COHEN, Solid State Commun. 8, 627 (1970).
M. WELCOWSKY and R. BRAUNSTEIN, Phys. Rev. B 5, 497 (1972).
[25] R. C. CHANEY, C. C. LIN, and E. E. LAFON, Phys. Rev. B 3, 459 (1971).
[26] D. E. ASPNES and A. A. STUDNA, Solid State Commun. 11, 1375 (1972).
[27] S. CIRACI and I. P. BATRA, Phys. Rev. B 15, 4923 (1977).
[28] G. D. WATKINS and R. P. MESSMER, in: Computational Methods for Large Molecules and Localized States in Solids, Ed. F. HERMAN, A. D. MCLEAN, and R. K. NESBET, Plenum Press, New York 1973 (p. 133).
[29] H. J. MCSKIMIN, J. appl. Phys. 24, 988 (1953).
[30] E. G. SIEVERTS, Thesis, Univ. Amsterdam, 1978 (unpublished).

(Received May 17, 1979)